Plasma Parameters of a Gliding Arc Jet at Atmospheric Pressure Obtained by a Line-Ratio Method

2013 Plasma Sci. Technol. 15 776

(http://iopscience.iop.org/1009-0630/15/8/11)

Plasma Parameters of a Gliding Arc Jet at Atmospheric Pressure Obtained by a Line-Ratio Method*

LI Hui (李辉)[1], XIE Mingfeng (谢铭丰)[2]

[1]Department of Thermal Science and Energy Engineering, University of Science and Technology of China, Hefei 230027, China
[2]National Synchrotron Radiation Laboratory, University of Science and Technology of China, Hefei 230029, China

Abstract A generator of the gliding arc jet (GAJ), which is driven by a transverse magnetic field, is developed to produce non-equilibrium plasma at atmospheric pressure. The gas temperature is estimated using the spectrum of OH radicals to be about 2400±400 K. The determinations of electron temperature and electron density by using a line-ratio method are elaborated for the gliding arc jet plasma. This line-ratio method is based on a collisional-radiative model. The experiment results show that electron temperature is about 1.0 eV and electron density is about 6.9×10^{14} cm^{-3}. Obviously, the plasma of GAJ is in a non-equilibrium state.

Keywords: GAJ, line-ratio method, collisional-radiative model (CRM)

PACS: *52.80.Mg, 52.70.Kz*

DOI: 10.1088/1009-0630/15/8/11

1 Introduction

Non-thermal and low temperature plasmas, especially in an open environment/atmosphere (∼1 atm), are of great interest in different fields of science and in applications such as methane steam reforming [1,2], material processing [3,4], environmental protection [5,6], microbial decontamination [7,8] and other applications [9,10]. A gliding arc is a simple and cheap approach to produce non-equilibrium plasmas at atmospheric pressure. It can provide high power for a high productivity reactor with high energy efficiency and high selectivity for chemical reactions [11,12]. It has been applied in many of the above-mentioned fields.

The gliding arc can generate weakly ionized plasma between two horn-shaped electrodes. It can be driven by a gas flow or a magnetic field [13∼15]. Plasma of the gliding arc can be in either an equilibrium state or a non-equilibrium state, depending on the system parameters such as power input and gas flow rate [14]. In most applications, the non-equilibrium state is required. Therefore, plasma parameters of the gliding arc at atmospheric pressure would be carefully investigated. But plasma parameters of the gliding arc in a non-equilibrium state are discussed only qualitatively or estimated indirectly by other parameters such as current density [16]. In a non-equilibrium state, plasma parameters can be measured by a Langmuir probe [17], microwave interferometer [18], laser Thomson scattering [19] and optical emission spectroscopy (OES) [20]. The OES technique, however, is a more appropriate method at atmospheric pressure due to its advantages of being non-intrusive, inexpensive and convenient. In this work, the gilding arc is mainly driven by a transverse magnetic field, and the injected argon flow is just diluted air. Plasma parameters of the gliding arc jet (GAJ) at atmospheric pressure are measured by a line-ratio method, which has been successfully applied to simultaneous determination of plasma parameters at both low- and high- pressure [21,22].

2 Experimental setup

Fig. 1(a) shows the experimental setups used in this paper. A transverse magnetic field (**B**), perpendicular to the arc current, is produced by the magnetic coil inside which an annular soft-iron core is set. There is a gap with a width of 12 mm left between the annular soft-iron core, and the left part of the annular soft-iron core is the N pole, the right one is the S pole. The magnetic induction in this gap could be controlled by adjusting the magnetic coil current. In this paper, the magnetic induction is set at about 4000 Gs while the magnetic induction outside the gap is negligibly small. The direction of the magnetic field in this gap is shown in Fig. 1(b). In order to observe the arc plasma inside this gap, a slit, whose width is about 2 mm, is left between S poles of the magnet. The transverse magnetic field is mainly used to drive the moving arc upwards.

The generator of the GAJ, which is placed in air, mainly consists of two copper electrodes as shown in Fig. 1(b). The left electrode is negative, and the right one is positive. The narrowest gap between the electrodes is about 1.5 mm. Two electrodes, whose thicknesses are about 2 mm, are set between one rectangle

*supported by National Natural Science Foundation of China (Nos. 10975136, 11035005) and USTC-NSRL Association Funding of China (No. KY2090130001)

ceramic slab (100 mm×74 mm×1 mm) and a piece of quartz glass. The generator of the GAJ is placed in the gap between the annular soft-iron cores. The gas injected into the generator is argon, which is mainly used to dilute air in the generator. The flow rate of argon is about 3.3 L/min.

The power is supplied by a DC high-voltage power source with an internal resistor (r_0) of about 688 Ω, and an open circuit voltage (V_0) of about 4.5 kV. The self-inductance is about 7 H. When the high-voltage supply is switched on, the gliding arc is first struck at the narrowest gap between the electrodes. Then the arc moves up driven by the magnetic field, and the arc voltage increases accordingly. When the high-voltage supply could not sustain the increasing arc voltage, the gliding arc would be extinguished, and the next discharge cycle begins.

The signals of arc voltage and arc current are sampled from electric resistances R_1(20 MΩ) and R_2(1 Ω), respectively. Then the signals are recorded by a four-channel digital storage oscilloscope (TDS2014, 100 MHz, 1 GS/s), and the electric waveforms are transferred to the PC for data processing. The observation point, where we measure plasma parameters of GAJ, is located at the midline between the two electrodes, and above the soft-iron core. The distance between the observation point and the narrowest gap of two electrodes is about 75 mm, as shown in Fig. 1(b).

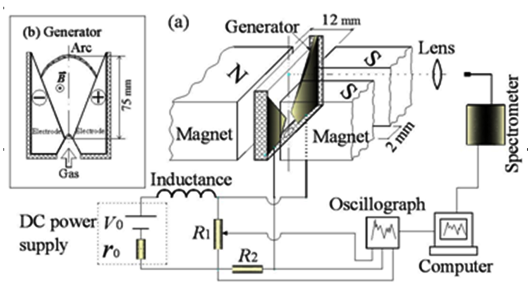

Fig.1 (a) A schematic diagram of the experimental device, (b) A generator of GAJ (color online)

The optical signals of plasma from the observation point are collected by an optical fiber with a collimating lens. Then the optical signals are recorded by a spectrometer (AvaSpec-2048-USB2-RM, resolution ~0.13 nm) through the optical fiber. The spectrometer has been calibrated by the Avantes corporation. The measured emission intensity by the spectrometer is actually a spatial integration of emissivity of the plasma along the line-of-sight. Because the gliding arc is moving continuously and its radius is commonly very small and about 1~2 mm, the spatial and temporal resolution of plasma properties is very difficult to be done. In this work, the emissivity of plasma is approximately considered as a constant. Therefore, all plasma parameters obtained by analyzing spectra are considered as average levels of plasma parameters of GAJ along the line-of-sight. In order to reduce the measurement errors caused by the motion of the gliding arc, each spectrum obtained had been averaged 100 times automatically by the spectrometer. At the same time, each measurement of the spectrum is repeated ten times. The intensities of ten measured spectra are perhaps different. As we know, when the arc column center coincides with the axis of the collimating lens, the intensity of the optical signal obtained by the spectrometer is the maximum. So we choose the maximum of ten spectra for analyzing.

3 Results and discussion

3.1 Gas temperature

The emission spectrum of argon in a UV band (i.e. 300~400 nm) under our experimental conditions is very complicated. The spectrums of OH(A-X), N_2(C-B), N_2^+(B-X), NH(A-X) and CN often overlap with each other. However, the spectrum of OH in 306~310 nm is almost isolated from the spectrum of N_2(C-B). The OH band ($A^2\Sigma$, $\nu = 0 \rightarrow X^2\Pi$, $\nu' = 0$) is used in our experiment, and the typical OH radical spectrum measured in the UV band of 306~310 nm is shown in Fig. 2. The emission spectrum of the OH radical is easily found in the discharge. If the signal noise ratio is low, it can be greatly improved by adding a little water into the injected gas. The typical OH spectrum measured is fitted by the least-square method based on the reference data of OH [23]. The fitting curve of the OH spectrum is also presented in Fig. 2. The rotational temperature of the OH radical is obtained by fitting and is about 2400 K, and the measurement error is about ±400 K. In this work, the rotational temperature of the OH radical is chosen for the estimation of gas temperature [20].

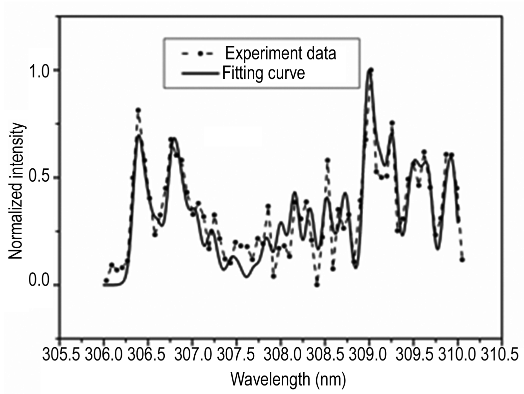

Fig.2 Typical measured spectrum of the OH radical (solid circles) and fitting curve (solid line)

3.2 Determinations of plasma parameters

For a non-equilibrium plasma, the population distribution of the excited levels of neutral atoms in plasma always deviate from the Boltzmann distribution. The routine method of analyzing atomic emission spectra, e.g. the Boltzmann plot, will not be able to obtain the kinetic electron temperature. A line-ratio method can be applied to the non-equilibrium plasma. This method measures certain spectral line intensities to get the intensity ratios, and then compares them with the same ratio values obtained from numerical simulations. These calculated line intensity ratios are obtained from the population densities of excited level atoms, which are calculated from the collisional radiative model (CRM). So a simple CRM, developed by ZHU and PU [24], is adopted here to calculate the densities of excited level argon atoms. This CRM takes into account 17 excited effective levels and 21 particle species. The main kinetic processes included in this model are electron impact excitation and de-excitation, atom collision excitation and de-excitation, electron-impact ionization, Penning ionization, electron collisional recombination for atomic and molecular ions, 3-body collisional association reactions, electron-impact and atom-collisional dissociations reactions, effective spontaneous radiative transitions between the effective levels, and the radiation from the excited molecules. The diffusion of the excited atoms and the ions to the wall is also included in this model. The population densities of ten 2p (Paschen's notation) levels atoms calculated by using this CRM under the same experimental conditions are found to fit well with the experimental results [24].

In experiments, the emission spectral lines of transition from 2p to 1s (Paschen's notation) are measured. So, we adopt this CRM to determine the population densities of 2p levels atoms under our experimental conditions. For one emission spectral line, the relationship between the population density (N_n) of a 2p level and the corresponding radiative intensity (I_n) of the emission spectral line is

$$\frac{N_n}{g_n} \propto \frac{I_n \lambda_n}{A_n g_n}, \tag{1}$$

where g_n is statistical weight of a 2p level, A_n is spontaneous transition probability and λ_n is wavelength. For two emission spectral lines, the population density ratio (R_{nm}) of two corresponding 2p levels is

$$R_{nm} = \frac{N_n/g_n}{N_m/g_m} = \frac{I_n \lambda_n / A_n / g_n}{I_m \lambda_m / A_m / g_m}. \tag{2}$$

If the intensity ratio (I_n/I_m) of two atomic emission lines is measured, the density ratio can be obtained. Therefore, the electron temperature and electron density can be determined from the comparison between the measured density ratio and the density ratio calculated by CRM. But we must notice that the calculated density ratio obtained from CRM is a function of both electron temperature and electron density. By using the line-ratio method to determine plasma parameters [21,25,26], we must pick out those density ratios that are sensitive only to one plasma parameter while not being sensitive to the other plasma parameters. So the spectral lines should be carefully selected.

Fig. 3 and Fig. 4 show the variations of four calculated density ratios of $2p_1/2p_4$, $2p_1/2p_7$, $2p_{10}/2p_9$ and $2p_8/2p_9$ in a certain range of electron temperature and electron density. The density ratios of $2p_1/2p_4$ and $2p_1/2p_7$ vary largely with electron temperature, but they vary little with electron density. So they are suitable for the determination of electron temperature. In contrast, the density ratios of $2p_{10}/2p_9$ and $2p_8/2p_9$ change largely with increasing electron density, and change little with electron temperature. So they are suitable for electron density determination. We choose eight argon atomic lines of 750.39 nm, 794.82 nm, 750.39 nm, 810.37 nm, 912.30 nm, 811.53 nm, 842.46 nm and 912.30 nm for plasma parameter determination. Line intensity ratios of $I_{750.39}/I_{794.82}$ and $I_{750.39}/I_{810.37}$ are used for electron temperature determination. But two different values of electron temperature will be obtained from two line ratios of $I_{750.39}/I_{794.82}$ and $I_{750.39}/I_{810.37}$ due to the errors from experimental measurements and numerical calculation of density ratios. If not for these errors, the electron temperature obtained from two line ratios of $I_{750.39}/I_{794.82}$ and $I_{750.39}/I_{810.37}$ should be the same. In order to increase the accuracy, the average of the results obtained from the two line ratios of $I_{750.39}/I_{794.82}$ and $I_{750.39}/I_{810.37}$ is taken as the final result of electron temperature (T_e). For the determination of electron density, the line intensity ratios of $I_{912.30}/I_{811.53}$ and $I_{842.46}/I_{912.30}$ are used. The average of the results obtained from the two line intensity ratios of $I_{912.30}/I_{811.53}$ and $I_{842.46}/I_{912.30}$

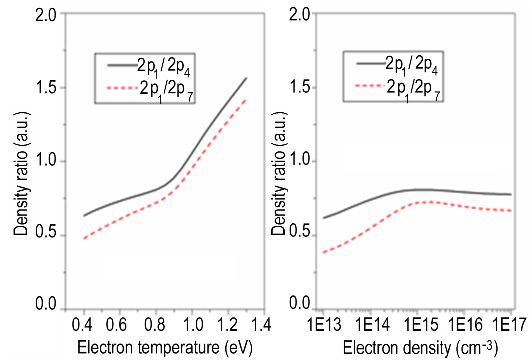

Fig.3 Two density ratios of $2p_1/2p_4$ and $2p_1/2p_7$ as functions of electron temperature and electron density (color online)

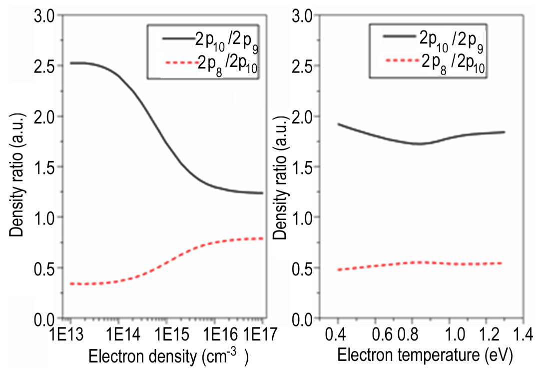

Fig.4 Two density ratios of $2p_{10}/2p_9$ and $2p_8/2p_9$ as functions of electron density and electron temperature (color online)

Table 1. Comparison of the properties between different types of discharges

Parameter	GAJ	MSGAD [16]	Thermal arc [16]
Gas temperature (K)	2400±400	2200∼2500	≫10000
Electron temperature (eV)	1.0	1.1∼0.8	1∼5
Electron density (10^{14} cm^{-3})	6.9	0.1∼3	$10^2 \sim 10^5$

is taken as the final result of electron density (N_e). From the measured atomic line spectra of argon, the plasma parameters obtained by the line-ratio method are T_e = 1.0 eV and $N_e = 6.9\times10^{14}$ cm^{-3}. The measurement error comes mainly from the numerical calculation of the density ratios, which are determined by the accuracy of the rate coefficients used in the rate balance equations of CRM. The uncertainty of the rate coefficients is generally 10%∼30% [27], which can lead to an uncertainty of 20%∼50% for electron temperature determination and an uncertainty of 30%∼60% for electron density determination.

From the plasma parameters measured above, the plasma of GAJ is obviously in a non-equilibrium state. However, it is difficult to compare our results with those of other papers, because the experimental conditions are to some extent different. We only collect plasma parameters from three types of discharges, and summarize them in Table 1 for a preliminary comparison. The plasma parameters of the GAJ and MSGAD have the same order of magnitude within the uncertainty. Gas temperature and electron density of the GAJ are less than those of the thermal arcs.

4 Conclusion

A generator of the gliding arc jet, which is driven by a transverse magnetic field, is developed to produce non-equilibrium plasma at atmospheric pressure. The gas temperature is estimated by using the spectrum of OH radicals. The determinations of electron temperature and electron density of plasma of GAJ by a line-ratio method are elaborated. This line-ratio method is based on a collisional-radiative model. The experiment results obtained by the line ratio method are T_e = 1.0 eV and $N_e = 6.9\times10^{14}$ cm^{-3}. Obviously, the plasma of GAJ is in a non-equilibrium state. Compared with other types of discharges, the plasma parameters of GAJ have the same order of magnitude as those of MSGAD.

Acknowledgements

The authors thank X M ZHU and Y K PU's group and Dr. Hiroshi AKATSUKA for help with the construction of a collisional-radiative model.

References

1 Durka T, Stefanidis G D, Van Gerven T, et al. 2011, International Journal of Hydrogen Energy, 36: 12843

2 Rafiq M H, Hustad J E. 2011, Ind. Eng. Chem. Res., 50: 5428

3 Janca J, Czernichowski A. 1998, Surface and Coatings Technology, 98: 1112

4 Yang R, Zheng J, Li W, et al. 2011, J. Phys. D: Appl. Phys., 44: 174015

5 Vandenbroucke A M, Morent R, Nathali D G, et al. 2011, Journal of Hazardous Materials, 195: 30

6 Krawczyk K, Mlotek M. 2001, Applied Catalysis B: Environmental, 30: 233

7 Ehlbeck J, Schnable U, Polak M, et al. 2011, J. Phys. D: Appl. Phys., 44: 013002

8 Soukayna L, Michael K, Emmanuel O. 2011, Advanced Materials Research, 324: 469

9 Tomohiro N, Gutsol A. 2011, J. Phys. D: Appl. Phys., 44: 270301

10 Lu X, Xiong Z, Zhao F, et al. 2009, Appl. Phys. Lett., 95: 181501

11 Fridman A, Nester S, Kennedy L A, et al. 1999, Progress in Energy and Combustion Science, 25: 211

12 Czernichowski A. 1994, Pure & Appl. Chem., 66: 1301

13 Richard F, Cormier J M, Pellerin S, et al. 1996, J. Appl. Phys., 79: 2245

14 Ozlem M Y, Saveliev A V, Fridman A A. 2000, Journal of Applied Physics, 87: 1632

15 Li H, Wang C B, Tao X P. 2007, Plasma Science and Technology, 9: 596

16 Gangoli S P, Gutsol A F, Fridman A A. 2010, Plasma Sources Sci. Technol., 19: 065004

17 Dickson S, Robertson S. 2010, Physics of Plasmas, 17: 033508

18 Hebner G A, Barnat E V, Miller P A, et al. 2006, Plasma Sources Sci. Technol., 15: 879

19 Muraoka K, Kono A. 2011, J. Phys. D: Appl. Phys., 44: 043001

20 Laux C O, Spence T G, Kruger C H, et al. 2003, Plasma Sources Sci. Technol., 12: 125

21 Zhu X M, Pu Y K. 2007, J. Phys. D: Appl. Phys., 40: 2533

22 Kissovski Z, Ivanov A, Iordanova S, et al. 2011, J. Phys. D: Appl. Phys., 44: 205203

23 Dieke G H, Crosswhite H M. 1961, J. Quant. Spectrosc. Radiat. Transfer., 2: 97

24 Zhu X M, Pu Y K. 2010, J. Phys. D: Appl. Phys., 43: 015204

25 Boffard J B, Lin C C, DeJoseph Jr C A. 2004, J. Phys. D: Appl. Phys., 37: R143

26 Donnelly V M. 2004, J. Phys. D: Appl. Phys., 37: R217

27 Zhu X M, Pu Y K. 2009, J. Phys. D: Appl. Phys., 42: 182002

(Manuscript received 18 May 2012)
(Manuscript accepted 15 August 2012)
E-mail address of LI Hui: huilli@ustc.edu.cn